

## Predissociation of the $B^3\Sigma_u^-$ state of $S_2$

Martyn D. Wheeler, Stuart M. Newman, and Andrew J. Orr-Ewing<sup>a)</sup>

*School of Chemistry, University of Bristol, Cantock's Close, Bristol BS8 1TS, United Kingdom*

(Received 14 November 1997; accepted 21 January 1998)

Predissociation of the  $B^3\Sigma_u^-$  state of  $S_2$  has been investigated by a combination of cavity ring-down spectroscopy and model calculations. The experimental spectra of the  $B^3\Sigma_u^- - X^3\Sigma_g^-(v',0)$  bands for  $10 \leq v' \leq 22$  span the wavenumber range 35 480–39 860  $\text{cm}^{-1}$ . Extensive variation is observed in the degree of rotational structure within the vibrational bands because of lifetime broadening caused by predissociation. Fits to the band contours give homogeneous linewidths for transitions to the  $B$ -state vibrational levels for  $10 \leq v' \leq 17$  that vary from  $\leq 1 \text{ cm}^{-1}$  for the (10,0) band to  $7 \pm 1 \text{ cm}^{-1}$  for the (17,0) band with a maximum linewidth of  $14 \pm 1 \text{ cm}^{-1}$  for the (13,0) band. For  $v' \geq 18$ , all bands are completely diffuse, indicating linewidths in excess of  $15 \text{ cm}^{-1}$ . The experimental results are compared with the results of a theoretical model that uses a Rydberg–Klein–Rees (RKR) potential for the  $B^3\Sigma_u^-$  state, *ab initio* calculations of the repulsive potentials that cross the  $B$  state, and Fermi golden rule calculations of the predissociation rates for the different repulsive potentials. Minor adjustments to the *ab initio* potentials, and an estimate of the spin-orbit coupling between the bound and repulsive states enable us to calculate predissociation rates in excellent agreement with the experimental observations. We deduce that the predissociation for  $v' \leq 16$  is predominantly via a  $^1\Pi_u$  state, whereas for  $v' \geq 17$ , coupling to a second repulsive state, suggested to be either a  $^5\Sigma_u^-$  or  $^5\Pi_u$  state, provides the primary mechanism for predissociation.

© 1998 American Institute of Physics. [S0021-9606(98)00916-7]

### I. INTRODUCTION

The  $B^3\Sigma_u^- - X^3\Sigma_g^-$  system of  $S_2$  contains many bands spanning a wavelength range of 250–700 nm and is the  $S_2$  analog of the extensively studied Schumann–Runge band system of  $O_2$ .<sup>1</sup> Unlike  $O_2$ , however,  $S_2$  is not a stable molecule: it is produced only transiently in sulfur-containing flames and discharges,<sup>2–4</sup> and forms in high temperature ( $>800 \text{ K}$ ) sulfur vapor. The  $B^3\Sigma_u^- - X^3\Sigma_g^-$  transition is very intense and is responsible for the blue color arising from flames and discharges containing sulfur. Since the first observation of the  $B-X$  transition by Graham<sup>5</sup> many attempts have been made to interpret this heavily perturbed band system and only recently<sup>6–8</sup> has a full rotational analysis been carried out. A complete understanding of this band system is desirable for a number of reasons: for example, the strength of the transition makes laser induced fluorescence (LIF) detection of  $S_2$  a useful probe for studying combustion processes of sulfur-containing fossil fuels. The detection of  $S_2$  also provides a means of studying the elementary chemical dynamics of sulfur-containing species as it is a product of, for example,  $CS_2$  photolysis,<sup>9</sup> and reactions such as that of  $S(^1D) + OCS$ .<sup>10</sup>  $S_2$  was observed transiently in the atmosphere of Jupiter by the Hubble space telescope following the recent impact of the comet Shoemaker–Levy.<sup>11</sup> It has also been observed via the  $B-X$  transition within cometary atmospheres,<sup>12,13</sup> and has been implicated in the sulfur chemistry occurring within dense molecular clouds.<sup>14,15</sup> At high temperatures, the large number of bands in the  $S_2 B-X$  spectrum overlap to cause a virtual continuum of emission

throughout the ultraviolet (UV) and visible part of the spectrum: this transition has thus been proposed as an optically pumped, widely tunable (365–570 nm) chemical laser.<sup>16</sup> Mercury-free discharge lamps and daylight-simulation light bulbs using low-pressure radio-frequency sulfur discharges also rely on the emission on the  $S_2 B-X$  transition.<sup>17</sup>

The ground  $X^3\Sigma_g^-$  state of  $S_2$  arises from the electronic configuration  $\dots 5\sigma_g^2 2\pi_u^4 2\pi_g^2$ , and has been well characterized by a combination of electron paramagnetic resonance (EPR)<sup>18</sup> and microwave<sup>19</sup> studies. The  $a^1\Delta_g$  and  $b^1\Sigma_g^+$  states also arise from this configuration and both have been observed experimentally. The first excited molecular configuration  $\dots 5\sigma_g^2 2\pi_u^3 2\pi_g^3$  gives the  $B^3\Sigma_u^-$  state, which is the focus of this work, and another five possible excited electronic states,  $c^3\Sigma_u^-$ ,  $A'^3\Delta_u$ ,  $A^3\Sigma_u^+$ ,  $b^1\Delta_u$ , and  $^1\Sigma_u^+$ , the first four of which have been identified via spectroscopic transitions. The configuration  $\dots 5\sigma_g^2 2\pi_u^4 2\pi_g^1 5\sigma_u^1$  is also of importance in the current work since it gives rise to the  $B''^3\Pi_u$  and  $^1\Pi_u$  states. The former state is responsible for the extensive perturbations observed in the  $B$  state, with the dominant interaction being spin-orbit coupling, and has been identified spectroscopically.<sup>20–22</sup> The latter state has been invoked by several authors<sup>23,24</sup> to be responsible for the onset of the first predissociation in the  $B$  state for vibrational levels above  $v' = 9$ . The  $^5\Pi_u$  and  $^5\Sigma_u^-$  states, which have the respective principal occupations  $\dots 5\sigma_g^2 2\pi_u^2 2\pi_g^3 5\sigma_u^1$  and  $\dots 5\sigma_g^1 2\pi_u^4 2\pi_g^2 5\sigma_u^1$ , are also of relevance to the current study because of their possible roles in  $S_2 B^3\Sigma_u^-$  predissociation.

Much effort has been expended over the past 80 years to try to understand the extensively perturbed rotational structure of the  $B-X$  transition. The coarse vibrational energy

<sup>a)</sup>Electronic mail: a.orr-ewing@bristol.ac.uk

level structure of the  $B$  state is described by the currently accepted spectroscopic constants<sup>25</sup>  $T_e = 31\,835$ ,  $\omega_e = 434$ ,  $\omega_e x_e = 2.75\text{ cm}^{-1}$ . Early attempts to understand the perturbed nature of the  $B$  state mainly involved partial rotational analyses of isolated pairs of vibrational bands.<sup>26</sup> Many rotational perturbations were observed in vibrational levels  $v' = 7, 8$ . From the analyses, the nature of the perturbing state was deduced to be  ${}^3\Pi_u$  and was ascribed the spectroscopic label  $B''$ . Further studies<sup>27</sup> revealed erratic variation of the molecular constants with vibrational level, such as the spin–spin splitting constant ( $\lambda$ ) having values of  $\sim -4.7\text{ cm}^{-1}$  for  $v' = 0, 2, 4$  and  $\sim +9.5\text{ cm}^{-1}$  for  $v' = 1, 3, 5$ . Attempts have been made to provide a deperturbation model in terms of mixing between the  $B$  and  $B''$  states<sup>28,29</sup> in order to understand the observed rotational structure of the  $B$  state for  $0 \leq v' < 10$ . The most recent and thorough analysis<sup>6–8</sup> yielded deperturbed constants for levels up to  $v' = 9$  by using experimental results from both jet-cooled and room-temperature spectra.

In his original study of the absorption spectrum of the  $B-X$  band system, Graham<sup>5</sup> noted two regions where the lines became diffuse: the first beginning with the (11,0) band and the second with the (18,0) band. The first specific studies of predissociation effects within high vibrational levels of the  $B\ {}^3\Sigma_u^-$  state were conducted by Olsson,<sup>30</sup> and the phenomenon was further investigated by Herzberg and Mundie.<sup>31</sup> Prior to these studies it had been established that emission from the  $B\ {}^3\Sigma_u^-$  state abruptly breaks off at high rotational levels within the  $v' = 8$  and 9 levels, with no emission seen from the  $v' = 10$  level.<sup>32,33</sup> These and the observations of Herzberg and Mundie indicate a limit for predissociation lying somewhere between the  $v' = 9$  level (at high rotational excitation) and the origin of the  $v' = 10$  level. Herzberg attributed the predissociation mechanism to a type Ic case, i.e., the predissociation limit lies appreciably higher in energy than the true dissociation energy of the predissociating state, thereby giving an upper limit for the dissociation energy of  $S_2$  of  $D_0 = 35\,500\text{ cm}^{-1}$ . This result was contrary to the conclusions drawn from the work of Rosen *et al.*<sup>33</sup> who, from the breaking off in emission of bands with  $v' = 8$  and 9, assigned the predissociation as case Ib (with the crossing of the potentials lower than the dissociation energy of the predissociating state). Ricks and Barrow<sup>34</sup> reexamined predissociation within the  $B$ -state levels  $v' = 8, 9$ , and 10 carefully analyzed the breaking off in emission at the onset of predissociation for  ${}^{32}S_2$ ,  ${}^{34}S_2$ , and  ${}^{32}S^{34}S$ . They obtained three limiting curves of predissociation corresponding to the  $F_1$ ,  $F_2$ , and  $F_3$  components (only the  $F_1$  component was observed for  $v' = 10$ ), all of which extrapolated to the same limit of  $35\,999.0 \pm 2.5\text{ cm}^{-1}$  above the ground-state minimum. From their data, they estimated the energy of the crossing point,  $E_c$ , using the method of Herzberg, and interpreted the predissociation as case Ib. Therefore, the limiting value of predissociation,  $35\,999.0 \pm 2.5\text{ cm}^{-1}$ , should correspond to the true dissociation limit. Since the last value of  $J'$  observed in emission decreased with increasing vibrational level, Ricks and Barrow were able to assign the predissociation as type Ib<sup>+</sup> in Mulliken's classification, i.e., an outer wall crossing, thus eliminating the repulsive inner wall of the

$B''$  state as a candidate for the predissociating state. The limiting curves for predissociation of all three  $\Omega$ -components,  $F_1$ ,  $F_2$ , and  $F_3$ , of the  $B$  state tend toward the same limit, indicating that they were all predissociated by the same state. Ricks and Barrow postulated that the first predissociating state was a  $1_u$  state correlating with  $S({}^3P_2) + S({}^3P_1)$  and proposed the  ${}^1\Pi_u$  state as a likely candidate since it would be capable of predissociating all three  $\Omega$ -components of the  $B\ {}^3\Sigma_u^-$  state. By making use of the known spin-orbit splitting between  $S({}^3P_2)$  and  $S({}^3P_1)$  of  $396.8\text{ cm}^{-1}$ , they were also able to obtain an improved estimate of the ground-state dissociation energy,  $D_0 = 35\,216.4 \pm 2.5\text{ cm}^{-1}$ .

Emission from the lowest rotational levels of the  $B\ {}^3\Sigma_u^-$   $\Omega' = 0$ ,  $v' = 10$  level has recently been studied in detail,<sup>7,21</sup> and the lifetime calculated from fluorescence decay rates was less than 3 ns compared to a lifetime of 32 ns for lower, nonpredissociated vibrational levels. In these studies no emission was observed for  $v' > 10$ , although emission from  $v' = 10, 11$ , and 12 has been reported when  $S_2$  is formed from the reaction of H atoms with  $H_2S$  ( $v' = 10, 11$ )<sup>35,36</sup> and in an electrical discharge of  $SF_6/He$  mixtures ( $v' = 10, 11, 12$ ).<sup>37</sup> This emission is attributed to inverse predissociation, i.e., to atomic recombination and fluorescence in the absence of a third body quencher.

Theoretical investigations of the  $B\ {}^3\Sigma_u^-$  and higher lying states of  $S_2$  have, to date, been limited. Swope *et al.*<sup>38</sup> performed self-consistent-field (SCF) and configuration-interaction (CI) calculations using an augmented double-zeta basis set on 13 low-lying electronic states including the  $X\ {}^3\Sigma_g^-$ ,  $B\ {}^3\Sigma_u^-$ ,  $B''\ {}^3\Pi_u$ , and  ${}^1\Pi_u$ . From these calculations it was concluded that the  ${}^1\Pi_u$  state was weakly bound, lying at an energy of around  $37\,600\text{ cm}^{-1}$ , and dissociates into two ground-state sulfur atoms. More recently a complete theoretical study of the  $B-X$  and  $B''-X$  band systems, including calculation of transition dipole moments, was carried out by Pradhan and Partridge.<sup>39</sup> Wave functions and potentials were obtained via multireference configuration-interaction (MRCI) calculations. Oscillator strengths, transition probabilities, and radiative lifetimes were calculated and were all shown to be in good agreement with experimental data.

Most of the experimental and theoretical studies of the  $S_2\ B-X$  band system have focused on the lower lying, nonpredissociated vibrational levels. In this study, we concentrate on the predissociated levels above  $v' = 10$ . Prior to this work, only plate spectra existed of transitions to these higher vibrational levels; hence extraction of dynamical information such as predissociation rates from spectral linewidths has been largely nonquantitative. The nature of the second predissociation has received little attention, although Barrow and du Parc<sup>24</sup> attributed it to an inner wall predissociation (Mulliken's type  $c^-$ ) via the  $B''\ {}^3\Pi_u$  state. We have investigated the  $B-X$  band system of  $S_2$  over the range of excited-state vibrational levels  $10 \leq v' \leq 22$  using cavity ring-down spectroscopy (CRDS).<sup>40–42</sup> Together with this experimental investigation, we conducted complementary *ab initio* calculations to clarify the nature and ordering of the possible states responsible for the observed predissociations within the  $B$  state. The resultant *ab initio* potentials, an improved

RKR potential for the  $B$  state, and Fermi golden rule calculations of predissociation rates were used to estimate the strength of the interstate interactions and thus to rationalize the experimental observations.

## II. EXPERIMENT

The experimental arrangement used to record the CRD spectra of  $S_2$  has been described in detail elsewhere,<sup>43</sup> and we give here only the specific details pertinent to this study. Spectra were recorded of  $S_2$  formed in a flow system within a 1.5-m glass vacuum tube. Two high-reflectivity (HR) mirrors (2-m radius of curvature), located in adjustable mounts at the ends of the flow tube, formed the ring-down cavity, and light escaping from one of the mirrors was detected by a photomultiplier tube. Spectra of the  $B-X$  (10,0), (11,0), and (12,0) bands were recorded using the frequency-doubled output of a dye laser (Spectra Physics PDL-3) operating with Fluorecein 548 and pumped by the 532-nm output of a Nd:YAG laser (Quantel YG680). To record spectra of the  $(v',0)$  bands with  $v' = 13-22$ , the dye laser, operating with Coumarin 500, 540, and 540A dyes, was pumped with the 355-nm third harmonic of the Nd:YAG laser. The dye-laser fundamental was frequency doubled in a BBO or KDP crystal to generate the necessary UV light between 250 and 282 nm. Spectral calibration of the dye-laser fundamental was performed by simultaneously recording optogalvanic lines of neon excited in a hollow cathode discharge. To cover the complete spectral range of the experiments, two HR mirror sets were required, the first having maximum reflectivity at a central wavelength of 290 nm (Virgo Lightning Optical Corp.), and the second centered at 243 nm (Research Electro Optics). At the central wavelength for the high-reflectivity mirrors, the  $1/e$  ring-down time was typically 10  $\mu$ s. Absorption spectra were obtained by direct least-squares fitting of the logarithm of the exponential decay function to obtain the variation of the ring-down time with wavelength.

$S_2$  was produced in a continuous flow from a mixture of H atoms and  $H_2S$ . The H atoms were generated by passing a microwave discharge through  $H_2$  (BOC High Purity) flowing through a length of mullite tube. The efficiency of  $S_2$  production was increased by lightly coating the mullite tubing with a solution containing ortho-phosphoric acid, methanol, and water. Typically, pressures of 1.0–2.0 Torr of  $H_2$  were flowed continuously through the tubing, with the microwave generator operating at an input power of approximately 30–40 watts. The  $H_2S$  (Matheson 99.5% purity) was gradually introduced into the ring-down cell 5 cm upstream of the H-atom inlet. Care had to be taken when adding the  $H_2S$  so as to suppress the formation of particulate sulfur products within the ring-down cavity as these decreased the ring-down time and dirtied the mirrors. Typical operating pressures of  $H_2S$  for the spectra reported here were  $\sim 10$  mTorr.

## III. RESULTS

Using the CRDS apparatus, spectra were taken of the  $S_2$   $B^3\Sigma_u^- - X^3\Sigma_g^-(v',0)$  band system with  $v'$  ranging from 10 to 22 spanning a total wavelength range of 282–250 nm.

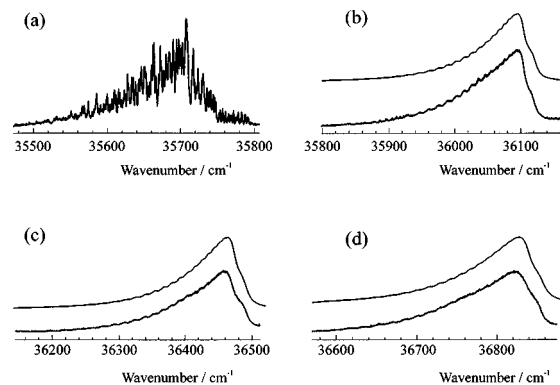


FIG. 1. CRDS spectra of vibrational bands of the  $S_2$   $B^3\Sigma_u^- - X^3\Sigma_g^-$  transition: (a) the (10,0) band; (b) the (11,0) band; (c) the (12,0) band; (d) the (13,0) band. Also shown in (b), (c), and (d), above the experimental spectra are spectral simulations obtained using the methods described in the text.

Levels with  $v' > 18$  are diffuse and completely unstructured and, for  $v' > 20$ , the experimental spectra showed only weak signals.

### A. $S_2$ $B^3\Sigma_u^-$ $v' = 10$

Figure 1(a) shows the CRDS spectrum of the  $B^3\Sigma_u^- - X^3\Sigma_g^-$  (10,0) band over the wavenumber range 35 480–35 800  $cm^{-1}$ . The LIF spectrum of this region shows the lowest  $J'$  (i.e.,  $J' = 1$ ) of the  $\Omega' = 0$  component, with other, higher  $J'$  levels appearing only weakly,<sup>7</sup> but the CRDS spectrum shows extensive rotational structure. Attempts were made to simulate this spectrum by extrapolating the deperturbed constants obtained from the previous vibrational bands seen in earlier, high resolution LIF studies.<sup>7</sup> Our attempts were, however, largely unsuccessful owing to strong rotational perturbations by the  $B'^3\Pi_u$  state, which are still evident in much of the spectrum: the  $B^3\Sigma_u^-$   $v' = 10$  level lies close to the dissociation limit of the  $B''$  state. A combination of our room-temperature spectrum and an ongoing fluorescence-depletion study<sup>44</sup> should clarify the observed structure. From our spectrum, however, we estimate full width at half maximum height (FWHM) values for the rotational linewidths  $\Gamma < 1$   $cm^{-1}$  since the spectrum clearly shows sharp structure: the homogeneous broadening results from predissociation and indicates a natural lifetime  $> 5$  ps. These linewidths should be compared with our instrument resolution, determined from previous studies<sup>45,46</sup> to be well described by a Gaussian function of FWHM 0.09  $cm^{-1}$ ; this instrumental resolution is limited by the UV laser linewidth. The estimates of  $S_2$   $B-X$  (10,0) linewidths and  $v' = 10$  lifetimes cannot be quantified more precisely because fitting to individual lines was prevented by the high density of overlapping rotational lines.

### B. $S_2$ $B^3\Sigma_u^-$ $v' = 11-22$

#### 1. Spectral linewidths

Figure 1(b) shows a CRD spectrum of the (11,0) band of the  $B-X$  transition over the wavenumber range 35 800–36 160  $cm^{-1}$ . It is clear from this spectrum that the predissociation is much more pronounced for  $v' = 11$  of the  $B^3\Sigma_u^-$  state than for  $v' = 10$ , since now the rotational fine

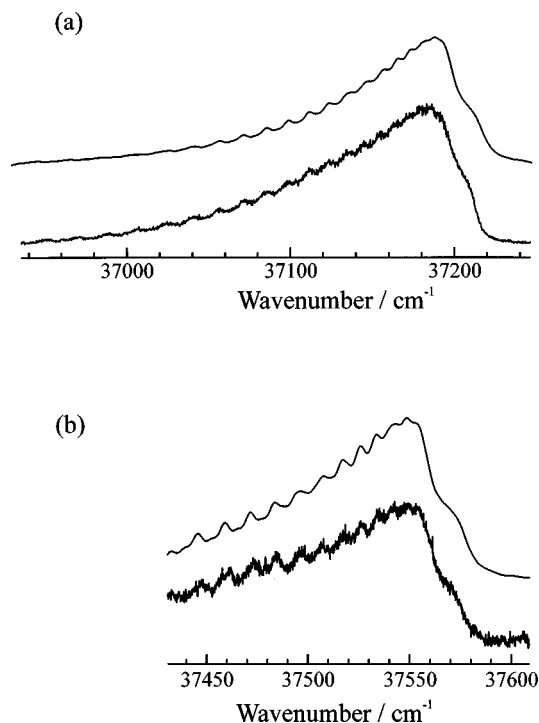


FIG. 2. CRDS spectra of vibrational bands of the  $S_2 B^3\Sigma_u^- - X^3\Sigma_g^-$  transition: (a) the (14,0) band; (b) the (15,0) band, together with spectral simulations obtained as described in the text.

structure is almost entirely washed away by homogeneous broadening, leaving only a small ripple on top of an almost continuous band profile. Also shown in the figure is a simulation of the  $B^3\Sigma_u^- - X^3\Sigma_g^-$  (11,0) band assuming a rotational temperature of 300 K. This simulation was derived using quoted literature values for the  $X^3\Sigma_g^-$  state constants<sup>6</sup> and modified values of the  $B$ -state constants deduced from a least-squares fitting procedure described in the next section. Along with the spectroscopic constants in the Hamiltonian matrix, the spectral linewidth (assumed independent of rotational quantum number and  $\Omega$ ) was included as a parameter

in the fitting procedure, with the broadening of the spectral lines described by a Lorentzian function with FWHM  $\Gamma$ . The spectral fits to the (11,0) band returned a value of  $\Gamma = 10 \pm 1 \text{ cm}^{-1}$  corresponding to a predissociative lifetime of  $530_{-50}^{+60}$  fs. The absence of marked structure in the spectrum meant that no rotational dependence for the linewidth could be deduced, and this lack of variation is reflected in the relatively large (10%) error in the estimated linewidth.

Figures 1(c), 1(d), 2, and 3 show CRD spectra of the  $B-X(v',0)$  bands with  $v' = 12 - v' = 19$ , together with simulations derived using the least-squares fitting procedure. All simulations assume a temperature of 300 K. It is evident from Fig. 1(c) that predissociation has become still more rapid at  $v' = 12$  of the  $B$  state since the rotational structure is even less pronounced than for the (11,0) band. The Lorentzian component of the spectral linewidth reaches a maximum FWHM value of  $14 \pm 1 \text{ cm}^{-1}$  at  $v' = 13$  [Fig. 1(d)], indicating a lifetime of  $380 \pm 30$  fs, though again there may well be some rotational dependence to this value which cannot be resolved in the spectrum. As the vibrational energy of the  $B$  state is increased beyond  $v' = 13$ , the rotational structure gradually becomes sharper and more pronounced, as is illustrated in Figs. 2 and 3, indicating that the rate of predissociation decreases for  $v' > 13$ . The signal-to-noise ratio is poorer in the spectrum of the  $B-X$  (15,0) band [Fig. 2(b)] than in the other  $B-X$  spectra and the spectrum is cut off at  $37\,430 \text{ cm}^{-1}$ ; the reason being that the reflectivities of both our mirror sets are comparatively low in this spectral region, therefore decreasing the ring-down time to less than  $1 \mu\text{s}$  and degrading the experimental sensitivity. The linewidth reaches a minimum value (for  $v' > 10$ ) of  $6 \pm 1 \text{ cm}^{-1}$  at  $v' = 16$  of the  $B$  state [Fig. 3(a)], and this linewidth corresponds to a predissociative lifetime of  $880_{-180}^{+60}$  fs. Again, we were unable to assess how the predissociation rates are affected by molecular rotation.

For excitation to vibrational levels above  $v' = 16$ , the FWHM of the Lorentzian lifetime-broadened component of the spectral line shapes once more increases: for  $v' = 17$

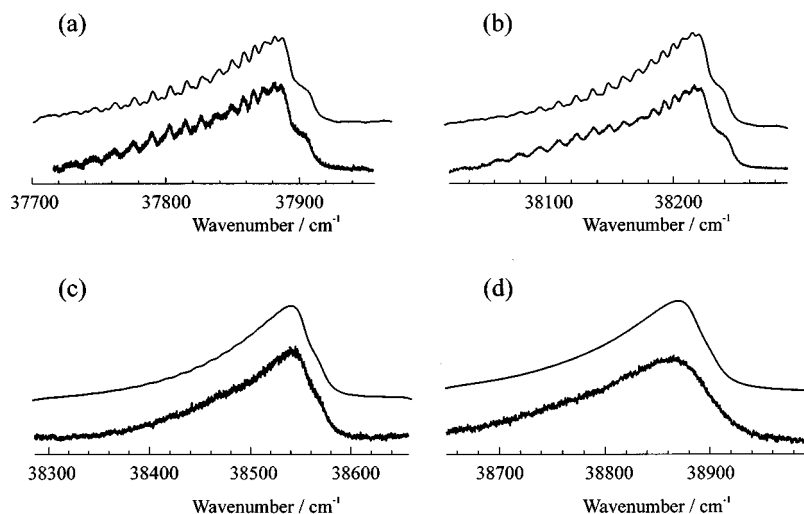


FIG. 3. CRDS spectra of vibrational bands of the  $S_2 B^3\Sigma_u^- - X^3\Sigma_g^-$  transition: (a) the (16,0) band; (b) the (17,0) band; (c) the (18,0) band; (d) the (19,0) band. Also shown, above the experimental spectra are spectral simulations obtained using the methods described in the text.

TABLE I. Values of the  $^{32}\text{S}_2 B^3\Sigma_u^-$  state constants and linewidths for the vibrational levels  $11 \leq v' \leq 19$  derived from the least-squares fitting procedure outlined in the text. All values are in  $\text{cm}^{-1}$ . Numbers in parentheses are the standard deviation ( $2\sigma$ ) of the parameters obtained from the fit.

$B^3\Sigma_u^- v'$	$T_v$	$B'_v$	$\lambda'_v$	$\Gamma_v$
10				$\leq 1$
11	36 109.9(3)	0.204(3)	1.3(4)	10(1)
12	36 477.4(5)	0.201(2)	1.5(5)	12(1)
13	36 843.3(7)	0.198(3)	1.7(4)	14(1)
14	37 201.0(6)	0.196(5)	1.9(4)	10(1)
15	37 563.5(6)	0.194(4)	2.2(3)	8(1)
16	37 896.7(5)	0.193(2)	2.4(2)	6(1)
17	38 230.9(4)	0.191(1)	2.7(4)	7(1)
18	38 558.9(7)			$> 15$
19	38 890(2)			$> 20$

[Fig. 3(b)]  $\Gamma = 7 \pm 1 \text{ cm}^{-1}$ , and for the (18,0) band [Fig. 3(c)], all rotational structure is lost and the band becomes diffuse, indicating linewidths in excess of  $15 \text{ cm}^{-1}$  (lifetime  $< 350 \text{ fs}$ ). For levels with  $v' > 18$ , the slight step at the start of the band (arising from transitions to the different  $\Omega$  components of the  $B$  state), which was clearly apparent in earlier spectra, is now lost, indicating that the bands become even more diffuse. Gradually the spectra become very weak and we did not look for bands with  $v' > 22$ . The linewidths derived from the least-squares fitting procedure for the  $B^3\Sigma_u^- - X^3\Sigma_g^-$  band progression  $10 \leq v' \leq 19$  are summarized in Table I.

## 2. Spectroscopic constants

The fits to the band contours for  $v' > 10$  give values not only for the spectral linewidths, but also for band origins, rotational constants, and spin-spin splitting constants. The fitting process was performed using the computer program PGOPHER,<sup>47</sup> in which adjustable parameters (the excited-state rotational constant,  $B'$ , the band origin,  $T_v$ , and the spin-spin splitting constant,  $\lambda'$ ) of a rigid-rotor Hamiltonian matrix, as well as the spectral linewidths, were floated in order to minimize the squares of the differences between the observed and calculated spectra. The ground-state constants were fixed at previously determined values.<sup>6</sup> Since the bands show no individually resolved rotational structure, the whole band contour was fitted until the total standard deviation reached a minimum. We were able to model the band contours successfully without the complications caused by the extensive perturbations evident for  $v' \leq 10$  because the predissociated bands lie well above the dissociation limit of the  $B''^3\Pi_u$  state. Derived values of the spectroscopic constants are shown in Table I and vary smoothly with vibrational level, confirming that the perturbations experienced in the lower part of the vibrational progression ( $v' \leq 10$ ) have switched off. The values of the constants obtained from the CRD experiment, together with deperturbed constants from Green and Western,<sup>6-8</sup> were used to obtain combined values for the equilibrium molecular constants  $T_e$ ,  $\omega_e$ ,  $\omega_e x_e$ ,  $B_e$ ,  $\alpha_e$ , and  $\gamma_e$  for the  $B$ -state levels extending from  $v' = 0$  to 19

TABLE II. Equilibrium values of molecular constants for the  $B^3\Sigma_u^-$  state of  $\text{S}_2$  derived from a weighted least-squares fit of the combined data for the  $v' = 11-20$  levels (this work) and  $v' = 0-9$  levels (from Refs. 6 and 7). Numbers in parentheses are the standard deviation ( $2\sigma$ ) of the parameters obtained from the fit. For comparison, literature values from experimental and theoretical studies are listed.

	Value ( $\text{cm}^{-1}$ )	Literature values ( $\text{cm}^{-1}$ )	
		Experimental <sup>a</sup>	Calculated <sup>b</sup>
$B_e$	0.2256(2)	0.2239	0.2234
$\alpha_e$	0.0014(2)	0.0023	0.001 98
$\gamma_e$	$-3.5 \pm 1.6 \times 10^{-5}$		
$T_e$	31 832.7(7)	31 835	31 826
$\omega_e$	435.2(3)	434.0	434.0
$\omega_e x_e$	2.72(2)	2.75	2.55

<sup>a</sup>Ref. 25

<sup>b</sup>Ref. 39.

(excluding  $v' = 10$ ). The latter three equilibrium constants relate to the rotational constants for the different vibrational levels via

$$B_v = B_e - \alpha_e(v + \frac{1}{2}) + \gamma_e(v + \frac{1}{2})^2. \quad (1)$$

We define  $T_e$  as the energy separation of the minima of the  $\Omega = 0$  components of the ground and excited states, consistent with previous authors.<sup>34</sup> Term values are obtained from  $T_e$  by adding the vibrational energy in the  $B$  state (from the potential minimum) and subtracting the  $X^3\Sigma_g^-$  state zero point energy of  $362.11 \text{ cm}^{-1}$  and a value of  $\frac{4}{3} \lambda = 15.78 \text{ cm}^{-1}$  corresponding to the ground-state spin-spin splitting.

The values of the equilibrium constants obtained from the above fitting procedures are given in Table II and for the purposes of comparison, previous values listed by Huber and Herzberg<sup>25</sup> and those calculated by Pradhan and Partridge<sup>39</sup> are included in the table. The values obtained here from the combination of our results and other recent work<sup>6-8</sup> differ slightly from the quoted literature values, reflecting in part the higher resolution and accuracy of the LIF<sup>6,7</sup> spectra compared to the original photographic-plate studies, and partly the nature of the deperturbation analysis used for  $v' \leq 9$ . The vibrational term values are reproduced to accuracies of  $\pm 6 \text{ cm}^{-1}$  by these constants, which is less than the experimental precision to which they can be determined because of incomplete deperturbation for  $v' \leq 9$ . Our objective in obtaining these equilibrium spectroscopic constants was to enable the construction of an RKR potential for the  $B^3\Sigma_u^-$  state, as discussed in the following section.

## IV. CALCULATION OF THE PREDISSOCIATION RATES

Given the detailed observations of the variation of linewidths over the wide range of vibrational levels ( $10 \leq v' \leq 22$ ) obtained from the CRDS experiments, we now seek to formulate a quantitative model in order to explain the nature of the predissociation mechanisms occurring in the high vibrational levels of the  $B^3\Sigma_u^-$  state of  $\text{S}_2$ . The calculations that make up the model were performed in two stages: first, detailed *ab initio* calculations were carried out to determine the ordering of states and characterize the  $R$ -dependence of

the possible repulsive potentials responsible for the predissociation. These repulsive potentials were then used together with an experimentally determined RKR potential for the  $B^3\Sigma_u^-$  state to perform Fermi golden rule calculations of the predissociation rates. A comparison of calculated and experimental rates enabled us to estimate the magnitudes of the spin-orbit interactions responsible for the predissociation.

### A. Determination of $S_2$ potentials

*Ab initio* potentials for the  $B^3\Sigma_u^-$  and  $B''^3\Pi_u$  states have been calculated previously,<sup>39</sup> but no such potentials were available in the literature for the higher, repulsive states with a sufficient degree of accuracy for our calculations of  $v'$ -dependent predissociation rates. We therefore undertook the necessary *ab initio* calculations of potential curves, including the  $B^3\Sigma_u^-$  and  $B''^3\Pi_u$  states, but restricted ourselves to states of ungerade symmetry since only these states have the appropriate symmetry for the predissociation of the  $B^3\Sigma_u^-$  state.<sup>48</sup>

The predissociating states must correlate to ground-state atomic fragments,  $S(^3P) + S(^3P)$ , whereas the  $B^3\Sigma_u^-$  state is correlated with the first excited atomic limit  $S(^3P) + S(^1D)$ . Consideration of the Wigner–Witmer correlation rules demonstrates that there are eight possible ungerade molecular states arising from the two ground-state atomic fragments, namely  $^1\Sigma_u^-, ^1\Pi_u, 2 \times ^3\Sigma_u^+, ^3\Pi_u, ^3\Delta_u, ^5\Sigma_u^-,$  and  $^5\Pi_u$ . The  $^1\Sigma_u^-, ^3\Sigma_u^+,$  and  $^3\Delta_u$  states are known from emission studies<sup>24</sup> to lie below the  $B^3\Sigma_u^-$  state and correlate with the  $^3P_2 + ^3P_2$  asymptote which lies  $35\,602\text{ cm}^{-1}$  above the  $X^3\Sigma_g^-$  state potential minimum.<sup>34</sup> The  $B''^3\Pi_u$  state also arises from the combination of two  $S(^3P)$  atoms but some questions still exist about which  $^3P_J$  spin-orbit components of the ground-state sulfur atoms this state correlates with. Recent observations<sup>7</sup> of  $B''$  state vibrational levels near to the  $S(^3P_2) + S(^3P_1)$  limit at  $35\,999\text{ cm}^{-1}$ , proposed by Ricks and Barrow<sup>34</sup> to be the dissociation limit of the first predissociating state, suggest that not all the  $\Omega$  components of the  $B''^3\Pi_u$  state converge to this limit; some are more likely to converge to the next highest atomic limit,  $S(^3P_2) + S(^3P_0)$  at  $36\,175\text{ cm}^{-1}$ . From these and other observations the correlation diagram for the ungerade states formed by  $S(^3P) + S(^3P)$  shown in Fig. 4 has been proposed.<sup>7,8</sup>

*Ab initio* calculations of these and some of the higher lying potentials identified in the correlation diagram were performed using the commercially available package of programs MOLPRO 96.<sup>49</sup> All the calculations used the correlation-consistent valence-quintuple-zeta (cc-V5Z) Gaussian basis set of Dunning and co-workers<sup>50</sup> and were carried out in  $D_{2h}$  symmetry. A restricted Hartree–Fock calculation was conducted in order to determine approximate forms for the ground-state molecular orbitals. These orbitals were then used as a first guess for calculating the excited-state wave functions and energies for a total of 21 internuclear distances (10 of which were concentrated in the region of the potential crossings between 2 and 3 Å) in a multireference configuration-interaction (MRCI)<sup>51,52</sup> calculation using complete active space SCF (CASSCF)<sup>53</sup> orbitals. Internal contraction of core orbitals was used and the effects of higher order excitations were accounted for by using the

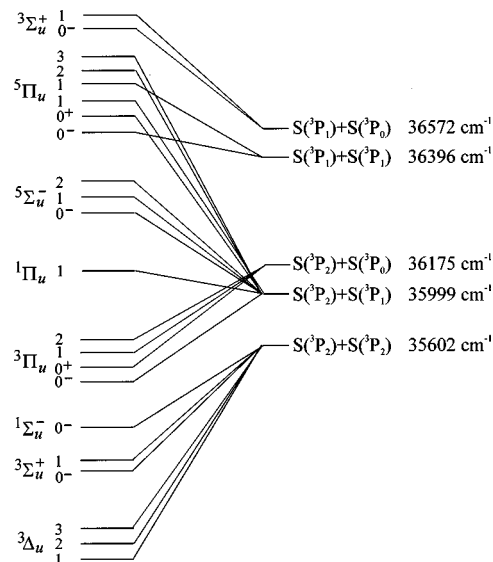


FIG. 4. Correlation diagram for the ungerade states arising from two  $S(^3P_J)$  atoms. The  $S(^3P_0) + S(^3P_0)$  asymptote is omitted because this combination gives rise to no ungerade states. The energies of the asymptotes are specified with respect to the base of the  $S_2X^3\Sigma_g^-$  potential well.

multireference analog of the Pople correction. Calculations were carried out on a Silicon Graphics SGI Power Challenge at the University of Bristol Computing Service.

The potential energy curves determined from the MRCI calculations, but shifted slightly in energy as described below, are shown in Fig. 5. The potential minimum of the  $X^3\Sigma_g^-$  state has been selected as the zero of energy and all other potentials are referenced from this point. The *ab initio* calculations do not take into account the effect of spin-orbit coupling and all eight calculated ungerade states arising from the  $S(^3P) + S(^3P)$  combination should therefore tend to the same asymptotic limit; the calculated asymptotic energies actually lie within  $880\text{ cm}^{-1}$  of one another. The calculations return a value for the separation of the  $S(^3P) + S(^3P)$  and  $S(^3P) + S(^1D)$  asymptotes of  $\sim 9050\text{ cm}^{-1}$  (taken from the mean of the calculated  $S(^3P) + S(^3P)$  energies for the various potential curves) compared to a value of  $9239\text{ cm}^{-1}$  derived from the known atomic energy levels of sulfur. For the

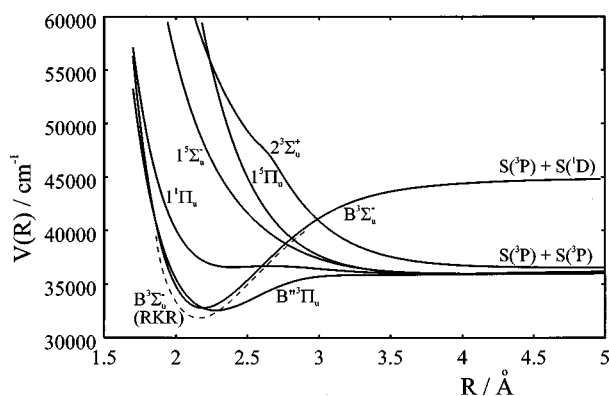


FIG. 5. *Ab initio* potential energy curves for the low-lying ungerade states of  $S_2$  relevant to this study. Also shown as a dashed line is the RKR potential for the  $B^3\Sigma_u^-$  state. The zero of energy is taken as the bottom of the  $X^3\Sigma_g^-$  potential well.

calculation of predissociation rates described later, it is important to correlate the repulsive molecular states with the correct atomic limits, as shown in Fig. 4, since different energetic asymptotes will result in different kinetic energies imparted to the dissociating atomic fragments and therefore affect the de Broglie wavelengths of the continuum wave functions. As we illustrate in Sec. V, the de Broglie wavelengths and the relative phases of the bound and continuum wave functions are important factors influencing the rates of predissociation of  $S_2 B^3\Sigma_u^- v'$  states. The energy separations of the  $^3P_1$ ,  $^3P_0$ , and  $^1D$  atoms from the  $^3P_2$  state of sulfur are 396.8, 573.6, and 9239.0  $\text{cm}^{-1}$ , respectively.<sup>54</sup> The *ab initio* potentials were shifted in energy so that their asymptotes were consistent with the energies of the proposed atomic correlations. Having modified the potentials in this way, we found that predissociation of the  $v'=10$  level of the  $B$  state was prevented by a small calculated maximum on the  $^1\Pi_u$  state potential: this potential shows a shallow minimum at  $R \approx 2.4 \text{ \AA}$  and a small maximum at  $R \approx 2.7 \text{ \AA}$ . We thus chose to position the  $^1\Pi_u$  potential curve such that the maximum lay just above the energy of the  $B^3\Sigma_u^- v'=10$  state, which entailed a vertical shift of the potential by  $-500 \text{ cm}^{-1}$ .

The ordering of the repulsive molecular states obtained from the *ab initio* calculations shown in Fig. V are consistent with the correlation diagram in Fig. 4 and follow the same pattern as is observed for the electronic states of  $O_2$ . The relative positions of the  $^5\Sigma_u^-$  and  $^5\Pi_u$  states are also in agreement with experimental evidence that implicates these states in mixing with the  $0_u^-$  component of the  $B''$  state, thereby accounting for the observation of  $^5\Sigma_g^-$  and  $^3\Pi_g$  ion-pair states of  $S_2$  from double-resonance studies.<sup>55</sup>

The *ab initio* potential for the  $B^3\Sigma_u^-$  state was not sufficiently precise for our subsequent calculations of predissociation rates which require accurate energies of the vibrational levels of the  $B$  state. We therefore constructed an RKR potential from the spectroscopic constants for the  $B^3\Sigma_u^-$  state listed in Table II using the computer program RKR1.<sup>56</sup> The  $B^3\Sigma_u^-$  RKR potential obtained extends as far as the energy of  $v'=20$  and is shown in Fig. 5, together with the *ab initio* potentials. The figure illustrates the accuracy of the *ab initio* calculations for such a complex, many-electron system, but the discrepancies between the RKR and *ab initio* values justify the modest corrections of the energies of the repulsive curves described above. Numerical integration of the radial Schrödinger equation for the  $B$ -state RKR potential using the program LEVEL<sup>57</sup> generated vibrational wave functions and energies; the energies were compared with experimental observations and were found to be accurate to within  $5 \text{ cm}^{-1}$  even for the higher vibrational levels ( $v' > 17$ ). The small discrepancies reflect the uncertainty with which the vibrational energy levels are calculated from the equilibrium molecular constants in Table II, and the RKR potential can be concluded to be a very good approximation to the true potential. Numerical values for the *ab initio* and RKR potentials used in this study can be obtained from the authors on request.<sup>58</sup>

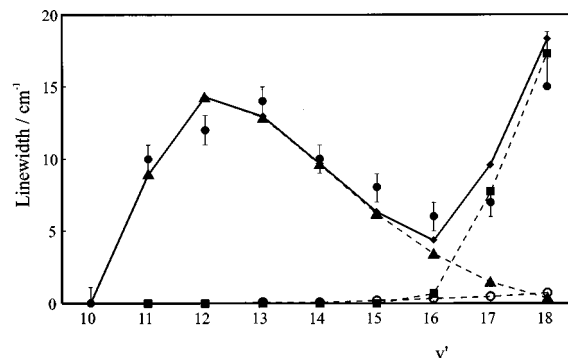


FIG. 6. Experimentally observed (●) variation of the linewidths of  $S_2 B^3\Sigma_u^- - X^3\Sigma_g^-(v',0)$  transitions with upper-state vibrational quantum number,  $v'$ . Also shown are the theoretically calculated linewidths obtained using the model described in the text for contributions to the predissociation from: ○ the  $B''^3\Pi_u$  state; ▲ the  $^1\Pi_u$  state; ■ the  $^5\Sigma_u^-$  state. The diamonds (◆) connected by the solid line show the sum of the calculated linewidths.

## B. Predissociation rates

Following the *ab initio* and RKR calculations of the  $S_2$  molecular potentials of ungerade symmetry described in the preceding section, we now concentrate on determining the contributions from each repulsive state to the observed predissociation rates of the  $B^3\Sigma_u^-$  state vibrational levels by estimating the magnitudes of the interstate spin-orbit interactions. A combination of potential curves and spin-orbit coupling functions permits Fermi golden rule calculations of the predissociation rates which can then be compared with our experimental results. Using the RKR  $B^3\Sigma_u^-$  state potential, together with the *ab initio* inner repulsive wall of the  $B''^3\Pi_u$  state bound potential and the  $^1\Pi_u$ , and  $^5\Sigma_u^-$  repulsive potentials, predissociation rates were calculated as a function of vibrational quantum number  $v'$  using the program BCONT.<sup>59</sup> The calculations were performed for each of the repulsive potentials individually in order to determine their relative contributions to the predissociation rates. For predissociation via the  $B''^3\Pi_u$  state, we extrapolate the results of a spectroscopic determination<sup>6,8</sup> of the  $R$ -dependence of the spin-orbit coupling to the  $B^3\Sigma_u^-$  state for  $v' \leq 9$ . To avoid introducing a complicated and arbitrary parametrization of the (unknown) spin-orbit coupling variation with internuclear separation for the  $^1\Pi_u$  and  $^5\Sigma_u^-$  states, however, we assume, for simplicity, a constant spin-orbit interaction independent of  $R$ . This approximation results in a model with just one adjustable parameter, the magnitude of the spin-orbit coupling between bound and repulsive states, and, as we show below, enables us to model the variation of the predissociation rates with  $v'$  in a simple fashion. The rates of predissociation are determined not only by the magnitude of the spin-orbit coupling between bound and repulsive states, but are also strongly affected by the degree of overlap between the bound vibrational wave functions and the continuum wave functions of the same energy.<sup>59</sup>

Figure 6 shows the results of our calculations of  $S_2 B^3\Sigma_u^-$  state lifetimes compared with our experimental data. The calculations were performed for zero rotational angular momentum ( $N'=0$ ) since, as discussed previously, we were unable to determine experimentally the rotational depen-

dence of the predissociation rates. Shown in the figure are the linewidths that would result for predissociation via the  $B''\ ^3\Pi_u$ ,  $^1\Pi_u$ , and  $^5\Sigma_u^-$  states individually; summing the calculated rates for each predissociative state and converting to homogeneous linewidths gives the total linewidth shown in the figure. It was found that the same general form of the variation of linewidth with  $v'$  was obtained in each case as  $N'$  increased, but that the actual magnitude varied only slightly compared to the total linewidth (by  $\sim 1-2\text{ cm}^{-1}$  as  $N'$  is increased to 40, corresponding to the tails of the vibrational bands in Figs. 1–3). This  $N'$  dependence is probably a consequence of a centrifugal contribution to the potential energy functions. An additional, rotation-dependent coupling mechanism may arise from the  $\mathbf{J}\cdot\mathbf{L}$  term in the Hamiltonian; previous analysis<sup>7</sup> suggests that at high  $J$  this term may give rise to a coupling amounting to about 10% of the magnitude of the spin-orbit coupling interaction described in the next section. Hence, we can discount substantial rotational effects in the analysis and concentrate on the variation of  $\Gamma$  with  $v'$ . We discuss in turn the contributions to the overall predissociation rate from the  $B''\ ^3\Pi_u$ ,  $^1\Pi_u$ , and  $^5\Sigma_u^-$  states as  $v'$  varies, and the magnitudes of the spin-orbit couplings between these states and the  $B\ ^3\Sigma_u^-$  state that are determined empirically so that the calculations correspond with the experimental measurements to the degree shown in Fig. 6.

### 1. The $B''\ ^3\Pi_u$ state

The  $B''\ ^3\Pi_u$  state can, in principle, contribute to the predissociation of the  $B\ ^3\Sigma_u^-$  state via an inner-wall coupling above the  $B''\ ^3\Pi_u$  state dissociation limit. To evaluate this contribution to the predissociation rate, we used the *ab initio*  $B''\ ^3\Pi_u$  potential to determine continuum wave functions. The magnitude of the spin-orbit coupling between the  $B\ ^3\Sigma_u^-$  and  $B''\ ^3\Pi_u$  states was taken from an experimental determination based on a deperturbation analysis of  $B$ - and  $B''$ -state vibrational levels below the predissociation limit.<sup>6</sup> The  $R$ -dependent coupling function derived from this analysis is of the form

$$H^{\text{SO}}(R) = a_1 + a_2(R - R_x) + a_3(R - R_x)^2, \quad (2)$$

where  $R_x$ , the internuclear separation about which the spin-orbit coupling function is expanded, was taken to be  $2\ \text{\AA}$ , and we assume the continued validity of this function above the dissociation limit of the  $B''$  state. The parameters  $a_1$ ,  $a_2$ , and  $a_3$  were derived by Green and Western<sup>6,8</sup> from a detailed fitting procedure and the resultant values are  $a_1 = 29.9\text{ cm}^{-1}$ ,  $a_2 = 187\text{ cm}^{-1}\ \text{\AA}^{-1}$ , and  $a_3 = 421\text{ cm}^{-1}\ \text{\AA}^{-2}$ . This spin-orbit coupling function results in an interaction energy of  $\sim 30-50\text{ cm}^{-1}$  at the inner wall of the  $B$  state at  $v' > 12$ . Using this coupling function and the  $B''$ -state *ab initio* potential, the calculated linewidths for the  $B$  state were determined to vary from  $0.002$  for  $v' = 10$  to  $0.98\text{ cm}^{-1}$  for  $v' = 19$ , thus making only a small contribution to the experimentally measured linewidths throughout the range of observed vibronic levels. We thus conclude that coupling to the  $B''\ ^3\Pi_u$  state is not the dominant mechanism of predissociation of the  $B\ ^3\Sigma_u^-$  state. Barrow and du Parc<sup>34</sup> suggested that the second predissociation limit of the  $B$  state arose because of the inner-wall crossing of this and the  $B''$  state,

and our calculations of the potentials confirm that the states do cross at an internuclear separation shorter than the equilibrium distance for the  $B$  state. The calculated rates, however, imply that the  $B''$  state is not responsible for the second onset of predissociation at  $v' > 16$ .

### 2. The $^1\Pi_u$ state

The  $^1\Pi_u$  state has been postulated as being responsible for the predissociation of the  $S_2\ B\ ^3\Sigma_u^-$  state via an outer-wall crossing in the region of  $v' = 11$ . A second predissociation limit could arise from an inner-wall crossing of the same two states at higher energy but our calculations suggest that this inner-wall crossing will occur at an energy well above the  $B$ -state dissociation limit. We are able to test the role of the  $^1\Pi_u$  state by comparing our experimental data for predissociation rates with calculated rates using our RKR and *ab initio* potentials for the  $B\ ^3\Sigma_u^-$  and  $^1\Pi_u$  states, respectively. For the interaction between these two states, no functional form for the variation with internuclear separation of the spin-orbit coupling between the states has been determined either theoretically or experimentally. As discussed above, we chose an approach intended to minimize the complexity of our model by limiting the number of parameters. We opted to use a constant value of  $H_{\text{SO}}$  independent of the internuclear separation, and we find that with an appropriate choice of the magnitude of the spin-orbit coupling, this simple model is sufficient to match the experimental observations.

As can be seen from Fig. 5, the gradient of the *ab initio*  $^1\Pi_u$  potential is quite flat in the region of the crossing point with the  $B\ ^3\Sigma_u^-$  state, and there is a shallow minimum at shorter internuclear distances ( $R \approx 2.4\ \text{\AA}$ ) followed by a low maximum at  $R \approx 2.7\ \text{\AA}$ . We suggest that the combination of these topographical features can explain the sudden jump in predissociation rate between  $v' = 10$  and  $11$ . The flatness of the repulsive potential has the effect of making the phase difference between the bound and continuum wave functions critically sensitive to the variation with internuclear separation of the steep repulsive wall, and this phase difference strongly influences the overlap of bound and continuum wave functions and hence the calculated predissociation rates. The  $^1\Pi_u$  potential was therefore moved both to shorter and longer  $R$  in an *ad hoc* fashion (though within a modest range about the calculated position) in order to reproduce the observed variation of predissociation rate with  $B$ -state vibrational level,  $v'$ . We found that the best fit with experimental observations, and in particular the observed trend of  $\Gamma$  with  $v'$ , was obtained by shifting the repulsive potential by  $0.07\ \text{\AA}$  to a larger internuclear distance. Once the correct form of the variation of predissociation rate with  $v'$  had been obtained, the magnitudes of the linewidths were modeled by tuning the strength of the spin-orbit coupling until calculated and experimental predissociation rates were in agreement. For the calculations shown in Fig. 6, an interaction energy of  $90\text{ cm}^{-1}$  was used, and this value clearly gives excellent correspondence between the observed and calculated (for  $N' = 0$ ) linewidths of all the studied vibrational levels up to  $v' = 16$ . If the *ab initio* potential without this  $0.07\ \text{\AA}$  correction (but with the energy adjustments described previously)

is used, the linewidth is found to oscillate more rapidly with vibrational level than is observed experimentally because of the effects of interference between bound and continuum wave functions. The overlap of the bound and continuum wave functions for our corrected potentials is discussed further and illustrated in Sec. V.

### 3. The ${}^5\Sigma_u^-$ state

As mentioned above, the inner-wall crossing of the  $B {}^3\Sigma_u^-$  and  $B'' {}^3\Pi_u$  states does not significantly enhance the calculated predissociation rate for  $v' > 16$  and the inner-wall crossing of the  $B {}^3\Sigma_u^-$  and  ${}^1\Pi_u$  states lies above the  $B$ -state dissociation limit. We propose that the second predissociation onset in the  $S_2 B {}^3\Sigma_u^-$  state, which leads to increased linewidths of transitions in the  $B {}^3\Sigma_u^- - X {}^3\Sigma_g^-$  spectrum for vibrational bands lying to shorter wavelengths than the (16,0) band, is a consequence of a second outer-wall crossing of the bound state by a repulsive potential in the vicinity of the energy of  $v' = 18$ . We therefore included the *ab initio*  ${}^5\Sigma_u^-$  repulsive potential in the model to account for the very strong predissociation occurring at around  $v' = 18$ . It is worth emphasizing that our *ab initio* calculations imply many interactions occurring in this region, as three repulsive curves cross the bound state in the region above the energy of  $v' = 18$  (see Fig. 5), all of which have several  $\Omega$  components. We thus use the  ${}^5\Sigma_u^-$  state as a representative example since it is calculated to cross the  $B$  state at an energy lower than the other states in this energy region. Our calculations do not demonstrate unequivocally that the state causing the second predissociation onset has  ${}^5\Sigma_u^-$  symmetry, but we use the results of our calculations for the  ${}^5\Sigma_u^-$  state as a sample potential curve to demonstrate that a repulsive potential of this form, lying at this energy, can explain the rapid predissociation of the  $B$  state for  $v' > 16$  using physically reasonable magnitudes for the spin-orbit coupling. As mentioned previously, the *ab initio*  ${}^5\Sigma_u^-$  potential curve was slightly shifted in energy to give the correct asymptotic limit for the  $S({}^3P_2) + S({}^3P_1)$  fragments.

To reproduce the experimental predissociation rates for  $v' > 16$ , we used a constant coupling strength between the  ${}^5\Sigma_u^-$  and  $B {}^3\Sigma_u^-$  states of  $100 \text{ cm}^{-1}$ , independent of the internuclear separation. As shown in Fig. 6, this interaction models the experimental observations very well and provides a satisfactory explanation of the second predissociation limit using a spin-orbit coupling interaction comparable to that required to model the first predissociation limit.

## V. DISCUSSION

The results of the calculations described in Sec. IV and summarized in Fig. 6 are in very good agreement with the experimentally observed variation of linewidths of  $B$ -state levels with  $v' \geq 10$ . The *ab initio* calculations give the form of the repulsive potentials but their energies must be shifted slightly to correlate asymptotically with the energies of the correct pairs of ground state sulfur atoms. The model explaining the predissociation mechanism is physically reasonable and contains very few adjustable parameters: the only adjustments to the *ab initio* potentials were to correct for the

$S({}^3P_2) + S({}^3P_1)$  asymptotes, and to fine-tune the crossing point of the  ${}^1\Pi_u$  potential with the  $B$  state; we also determined empirically the spin-orbit interaction matrix elements between the bound  $B {}^3\Sigma_u^-$  and repulsive  ${}^1\Pi_u$ ,  ${}^5\Sigma_u^-$  states. No rotational dependence for the predissociation rate can be inferred from the experimental observations and so all our calculations have been performed with  $N'$  set to zero. The  $N'$  dependence of the linewidth was investigated using the above model and we found that the effect of increasing  $N'$  is to cause the magnitude of the linewidths to become greater by  $\sim 10\% - 20\%$  of the observed values, while still retaining the same trend of variation with vibrational level. Having established a model for the predissociation of the  $B$  state, we now consider the details of the predissociation mechanism revealed by the model.

### A. Mechanism of the $B {}^3\Sigma_u^-$ state predissociation

With the extensive experimental observations given in Sec. III, and the description in Sec. IV of the predissociation occurring in high vibrational levels of the  $B {}^3\Sigma_u^-$  state of  $S_2$ , it is now possible to explain the mechanism in terms of interactions with the  $B'' {}^3\Pi_u$ ,  ${}^1\Pi_u$ , and  ${}^5\Sigma_u^-$  states. The latter two states are repulsive; the former state may cause predissociation via interaction with its repulsive inner wall above the dissociation limit to form  $S({}^3P) + S({}^3P)$ . We repeat the caution that although we refer to the highest lying of these states as the  ${}^5\Sigma_u^-$  state throughout, this choice of label is not supported by spectroscopic evidence and is based on the outcome of our *ab initio* calculations.

The first predissociation of the  $B {}^3\Sigma_u^-$  state, occurring slightly below  $v' = 10$ , can indeed be attributed to an interaction with a nearby  ${}^1\Pi_u$  state, in agreement with the original conjecture of Ricks and Barrow.<sup>34</sup> More recent studies<sup>7,21</sup> detected fluorescence only from the lowest rotational levels of  $B {}^3\Sigma_u^- \Omega' = 0 v' = 10$ . The fact that no  $B - X(10,0) \Omega' = 1$  transitions are observed in LIF lends support to the predissociation occurring via spin-orbit coupling with a  $1_u$  state, since the  $\Delta\Omega = 0$  selection rule ensures that only the  ${}^3\Sigma_u^- \Omega' = 1$  component of the  $B$  state can interact with the predissociating state for low rotational levels. Higher rotational levels of the  $B {}^3\Sigma_u^- \Omega' = 0 v' = 10$  state can predissociate by a  $J$ -dependent  $S$ -uncoupling interaction which effectively mixes  ${}^3\Sigma_{1u}^-$  character into the  ${}^3\Sigma_{0u}^-$  state as rotation is increased. In our room-temperature spectra, we may legitimately assume that all  $\Omega'$  components predissociate at almost the same rate, since this mixing of  $\Omega$  character sets in at low  $J$ . Calculations based on the model proposed in the current work suggest a homogeneous component of the linewidth of  $0.002 \text{ cm}^{-1}$  for transitions to  $v' = 10$ ,  $N' = 0$  corresponding to a lifetime for this level of 3 ns which is in very close agreement with the experimental fluorescence-lifetime measurements ( $< 3 \text{ ns}$ ).<sup>21</sup> The results of our minor modifications to the energies of the potential curves leave the  $v' = 10$  level just below the calculated crossing point of the  $B {}^3\Sigma_u^-$  and  ${}^1\Pi_u$  potentials. At shorter internuclear distances the (calculated)  ${}^1\Pi_u$  state has a shallow minimum at  $R \approx 2.4 \text{ \AA}$ , with a slight maximum at  $R \approx 2.7 \text{ \AA}$ . These features explain the slow onset of the predissociation since there will be very little overlap of the bound  $v' = 10$  and continuum

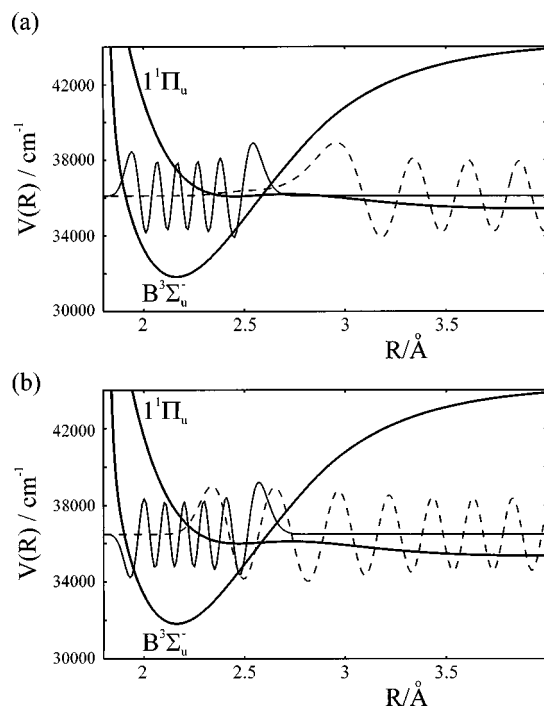


FIG. 7. Potentials and calculated  $B^3\Sigma_u^- v'$  (solid lines) and  $1^1\Pi_u$  state (dashed lines) wave functions of the same energy for: (a)  $v' = 10$ ; (b)  $v' = 11$ .

wave functions, as depicted in Fig. 7(a): the continuum wave function is much decayed in amplitude in the region of the curve crossing. This poor overlap in the region of the crossing, and hence weak predissociation, is contrary to the common observation of a rapid increase in the predissociation rates in the vicinity of a crossing between a bound and a steep repulsive potential, illustrated, for example, by our recent studies of SH  $A^2\Sigma^+$  predissociation.<sup>45,46</sup>

As the amount of vibrational excitation within the  $B$  state is increased, the degree of bound-continuum wave function overlap increases substantially as illustrated in Fig. 7(b) for  $B^3\Sigma_u^- v' = 11$ . The de Broglie wavelengths of the continuum wave functions, the phases of these and the bound wave functions, and, of course, the number of nodes in the bound wave function, change gradually with further vibrational excitation, causing the overlap to reach a maximum at  $v' = 13$ . For vibrational levels beyond  $v' = 13$  the overlap starts to decrease, causing the predissociation rate to become slower and resulting in a sharpening of the linewidth. As mentioned previously, if the  $1^1\Pi_u$  state is moved to slightly longer and shorter internuclear separation, the calculated predissociation rates oscillate in a very different fashion with  $v'$ , reflecting the sensitivity of the overlap of bound and continuum wave functions to the exact location of this repulsive state. The onset of the second predissociation occurs at around  $v' = 17$ , where the linewidths of the experimental spectra start to increase once more. In our model calculations, the lowest lying of the three repulsive states in this region, namely the  $5^5\Sigma_u^-$  state, was chosen to reproduce this second interaction. Figure 8 shows the calculated wave functions for the interaction of the  $B$  state with this  $5^5\Sigma_u^-$  state for  $v' = 17$  and 18. The substantial overlap of these wave func-

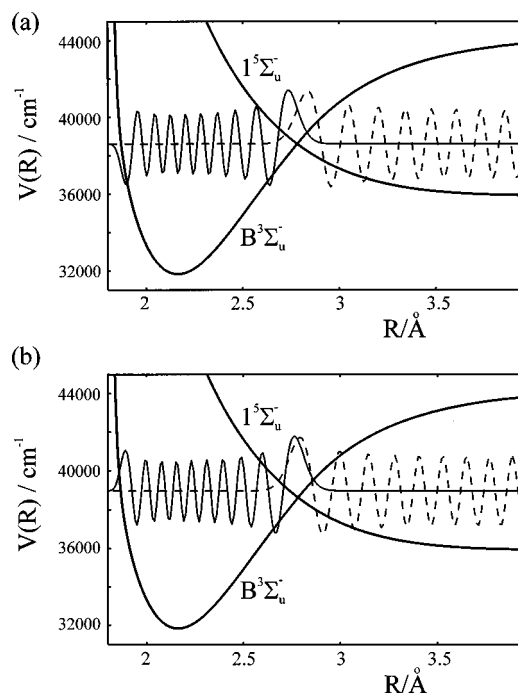


FIG. 8. Potentials and calculated  $B^3\Sigma_u^- v'$  (solid lines) and  $5^5\Sigma_u^-$  state (dashed lines) wave functions of the same energy for: (a)  $v' = 17$ ; (b)  $v' = 18$ .

tions is a likely cause of the sudden diffuseness in the spectrum for levels with  $v' \geq 18$ .

## B. Classification of the predissociation

The classification of the predissociation of the  $S_2 B^3\Sigma_u^-$  state has been the subject of much discussion, as outlined in Sec. I.<sup>31,33,34</sup> In light of our experimental and theoretical studies, we conclude that the strict classifications for both the first and second onsets of predissociation are type  $Ic^+$ , as was originally suggested by Herzberg in 1939.<sup>31</sup> The flatness of the  $1^1\Pi_u$  potential around its crossing point with the  $B$  state and the very shallow minimum at smaller internuclear distances, however, make this assignment arguable: the classification might be better expressed as intermediate between cases  $Ia^+$  and  $Ic^+$ . The predissociation limit is close to the dissociation limit of the predissociating state, though there is possibly a minor difference resulting from the small maximum on the  $1^1\Pi_u$  potential since tunneling through such a wide barrier is unlikely.

## C. Comparison with the predissociation of $O_2$ and $Se_2$

It is instructive to make a comparison of our deductions about the predissociation of the  $B^3\Sigma_u^-$  state of  $S_2$  with the well-characterized predissociations in the  $B$  states of the analogous, valence-isoelectronic systems  $O_2$  and  $Se_2$ . In  $O_2$ , the  $B^3\Sigma_u^-$  state is predissociated for levels above  $v' = 2$ ,<sup>60</sup> with a maximum linewidth of  $3 \text{ cm}^{-1}$  at  $v' = 4$ . This predissociation was originally attributed to a spin-allowed interaction with a  $3^3\Pi_u$  state.<sup>1,61</sup> A subsequent high resolution study, however, indicated that although the  $3^3\Pi_u$  state was responsible for some weak predissociations, the dominant pathway for predissociation to occur was via a spin-orbit interaction

with a  ${}^5\Pi_u$  state.<sup>60</sup> Other weak interactions responsible for predissociation in the Schumann–Runge band system were attributed to crossings with repulsive  ${}^1\Pi_u$  and  ${}^3\Sigma_u^-$  states. For  $v' \geq 5$ , a  ${}^3\Sigma_u^+$  state contributes to  $O_2$   $B$  state predissociation.<sup>62</sup> *Ab initio* calculations of the potential energy curves of  $O_2$  predict the  ${}^3\Pi_u$  state to cross the inner wall of the  $B$  state (case  $Ic^-$  predissociation) whilst the  ${}^5\Pi_u$ ,  ${}^1\Pi_u$ ,  ${}^5\Sigma_u^-$ , and  ${}^3\Sigma_u^-$  states all cross on the outer limb (case  $Ic^+$  predissociation).<sup>63</sup> The calculated ordering of states for  $S_2$  in Fig. 5 in this current study is exactly the same as that predicted by Schaefer and Miller<sup>63</sup> for  $O_2$ , but the crossings in the  $S_2$  system occur much higher on the  $B$ -state potential well. The spin-orbit interaction energy  $\langle {}^5\Pi_u | H^{SO} | {}^3\Sigma_u^- \rangle$  for predissociation in  $O_2$  has been calculated to be  $65 \text{ cm}^{-1}$ , indicating that the values of  $90\text{--}100 \text{ cm}^{-1}$  used in the calculations presented here for  $S_2$  are physically reasonable, as the spin-orbit coupling is expected to increase with atomic number [for  $O({}^3P_J)$  the  $J=2$  to  $J=1$  energy gap is  $158.5 \text{ cm}^{-1}$  whereas in  $S({}^3P_J)$  it is  $396.8 \text{ cm}^{-1}$ ]. We also note for comparison that in our calculations on the predissociation of SH  $A$   ${}^2\Sigma^+$ , the spin-orbit coupling values were close to  $100 \text{ cm}^{-1}$ .<sup>45,46</sup>

The currently accepted view of the predissociation of the  $O_2$   $B$  state is that a  ${}^5\Pi_u$  state is primarily responsible for the interaction,<sup>62</sup> and the  $S_2$   $B$  state is also crossed by a  ${}^5\Pi_u$  state. As shown by our calculations, it is quite feasible that the second predissociation of the  $S_2$   $B$  state is caused by interaction with a  ${}^5\Pi_u$  state rather than the  ${}^5\Sigma_u^-$  state we have invoked here, and hence we refrain from any definitive assignment of the nature of the electronic symmetry of this predissociating state pending calculations of the spin-orbit coupling to the  ${}^5\Pi_u$  and  ${}^5\Sigma_u^-$  states.

Predissociation of the  $B0_u^+$  state of  $Se_2$  by a  $0_u^+$  state is very strong and levels above the crossing point are so diffuse that they are not observed.<sup>64,65</sup> The perturbation responsible for the predissociation also manifests itself by causing large level shifts of the bound (sharp) levels. The maximum expected linewidth is estimated to be as much as  $140 \text{ cm}^{-1}$  at  $v' = 24$ . This predissociation is again caused by a spin-orbit interaction; this time the magnitude of the interaction is calculated to be  $373 \text{ cm}^{-1}$ , again lending support to our prediction of a matrix element of  $90\text{--}100 \text{ cm}^{-1}$  in  $S_2$ .

## VI. CONCLUSIONS

We have used the experimental technique of CRDS to characterize further and clarify the predissociation mechanisms occurring in the  $B$   ${}^3\Sigma_u^-$  state of  $S_2$  for  $v' \geq 10$ . In these experiments, homogenous line broadening of spectral lines was estimated from band contour fits to various  $(v',0)$  vibrational bands with  $v' = 10$  to  $19$  within the  $S_2$   $B$   ${}^3\Sigma_u^-$   $-X$   ${}^3\Sigma_g^-$  spectrum. The rotational lines of the  $(10,0)$  band have homogeneous components to their linewidths of  $\Gamma \leq 1 \text{ cm}^{-1}$  and the band shows sharp, as yet unassigned, rotational structure. All bands with  $10 < v' \leq 17$  show diffuse structure and vary in rotational linewidth from  $10 \pm 1 \text{ cm}^{-1}$  for the  $(11,0)$  band to  $7 \pm 1 \text{ cm}^{-1}$  for the  $(17,0)$  band, with a maximum linewidth of  $14 \pm 1 \text{ cm}^{-1}$  for the  $(13,0)$  band. All bands with  $v' \geq 18$  are completely diffuse, indicating the on-

set of a second strong predissociation at around  $v' = 18$  in the  $B$  state. For these bands only an estimate of a lower limit of  $15 \text{ cm}^{-1}$  for the linewidth is possible.

To complement this experimental study, we performed detailed *ab initio* calculations to understand the nature of the predissociating states, and, furthermore, have used the resultant calculated potentials together with an improved RKR potential for the  $B$   ${}^3\Sigma_u^-$  state to derive an analytical model that reproduces quantitatively the experimental data. The *ab initio* potentials were slightly shifted in energy to give the energies appropriate for the different  $S({}^3P_J)$  asymptotes. The model uses Fermi golden rule calculations of the predissociation rates to enable a comparison between theoretical predictions and our experimental measurements. The model indicates that the first predissociation, setting in at around  $v' = 10$ , is caused by a spin-forbidden interaction with a  ${}^1\Pi_u$  state which possesses a very shallow minimum at  $R \approx 2.4 \text{ \AA}$  (just inside the crossing point of the  $B$ -state potential). The observed form of the variation in linewidth with  $v'$  is reproduced if the whole *ab initio* repulsive potential is moved by  $0.07 \text{ \AA}$  to larger internuclear separation, and this variation is attributed to the rapidly changing overlap of bound and continuum wave functions. The magnitude of the spin-orbit interaction matrix element responsible for the predissociation is estimated to be  $90 \text{ cm}^{-1}$  and is taken to be independent of  $R$ . We suggest that the second predissociation is caused by one or more of a variety of states ( ${}^5\Sigma_u^-$ ,  ${}^5\Pi_u$ , or  ${}^3\Sigma_u^+$ ) since our calculations reveal that there are numerous crossings of the outer wall of the  $B$ -state potential at energies around and above the energy of the  $v' = 18$  level, and all of the states have more than one  $\Omega$  component. The observed behavior can be modeled successfully, however, if the lowest lying of these *ab initio* potentials, the  ${}^5\Sigma_u^-$  state, is treated as a single potential (hence neglecting the  $\Omega$  components) and an interaction energy of  $100 \text{ cm}^{-1}$  is invoked between it and the  $B$  state, independent of internuclear separation. A combination of the *ab initio*  $B''$ -state potential and a previously determined, experimentally derived  $B \sim B''$  spin-orbit coupling function enables us to conclude that coupling to the repulsive wall of the  $B''$  state constitutes at best only a very minor channel for predissociation of the  $B$  state. The theoretical model is unlikely to be the sole description of the predissociation behavior that accounts quantitatively for the observed rates. The model is attractive, however, because it contains a minimal number of adjustable parameters and the values of those parameters can be physically justified.

Future work will include refinements to the calculated potentials by extending the basis set and an *ab initio* calculation of the spin-orbit coupling matrix elements between the  $B$  state and the  $B''$   ${}^3\Pi_u$ ,  ${}^5\Pi_u$ ,  ${}^1\Pi_u$ , and  ${}^5\Sigma_u^-$  potentials for comparison with our predictions. Further analysis of the  $B-X(10,0)$  band using fluorescence-depletion experiments to clarify the rotational assignments is already underway.<sup>44</sup>

## ACKNOWLEDGMENTS

We thank Dr. C. M. Western and Professor M. N. R. Ashfold for many valuable discussions, and Dr. G. G. Balint-Kurti and Dr. S. H. Ashworth for assistance with the *ab*

*initio* calculations. We are grateful to K. N. Rosser for technical help, and to Professor R. J. Le Roy for the use of his programs. A.J.O.E. thanks the Royal Society for the award of the Eliz. Challenor Research Fellowship, and for additional funding for equipment. M.D.W. and S.M.N. thank, respectively, the University of Bristol and NERC for post-graduate studentships.

- <sup>1</sup>P. J. Flory, *J. Chem. Phys.* **4**, 23 (1936).
- <sup>2</sup>R. B. W. Pearse and A. G. Gaydon, *The Identification of Molecular Spectra* (Chapman and Hall, London, 1963).
- <sup>3</sup>A. Fowler and W. M. Vaidya, *Proc. R. Soc. London, Ser. A* **132**, 310 (1931).
- <sup>4</sup>G. Lakshminarayana and C. G. Mahajan, *J. Quant. Spectrosc. Radiat. Transf.* **16**, 549 (1976).
- <sup>5</sup>J. I. Graham, *Proc. R. Soc. London, Ser. A* **84**, 311 (1910).
- <sup>6</sup>M. E. Green and C. M. Western, *J. Chem. Phys.* **104**, 848 (1996).
- <sup>7</sup>M. E. Green and C. M. Western, *J. Chem. Soc., Faraday Trans.* **93**, 365 (1997).
- <sup>8</sup>M. E. Green, Ph.D. thesis, University of Bristol, 1996.
- <sup>9</sup>S. P. Sapers and D. J. Donaldson, *J. Chem. Phys.* **94**, 8918 (1990).
- <sup>10</sup>N. van Veen, P. Brewer, P. Das, and R. Bersohn, *J. Chem. Phys.* **79**, 4295 (1983).
- <sup>11</sup>K. S. Noll, M. A. McGrath, L. M. Trafton, S. K. Atreya, J. J. Caldwell, H. A. Weaver, R. V. Yelle, C. Barnet, and S. Edington, *Science* **267**, 1307 (1995).
- <sup>12</sup>S. J. Kim, M. F. Ahearn, and S. M. Larson, *Icarus* **87**, 440 (1990).
- <sup>13</sup>R. J. A. Grim and J. M. Greenberg, *Astron. Astrophys.* **181**, 155 (1987).
- <sup>14</sup>G. F. Mitchell, *Astrophys. J.* **287**, 665 (1984).
- <sup>15</sup>H. S. Liszt, *Astrophys. J.* **219**, 454 (1978).
- <sup>16</sup>S. R. Leone and K. G. Kosnik, *Appl. Phys. Lett.* **30**, 346 (1977).
- <sup>17</sup>N. D. Gibson, U. Kortshagen, and J. E. Lawler, *J. Appl. Phys.* **79**, 7523 (1996).
- <sup>18</sup>F. D. Wayne, P. B. Davies, and B. A. Thrush, *Mol. Phys.* **28**, 989 (1974).
- <sup>19</sup>H. M. Pickett and T. L. Boyd, *J. Mol. Spectrosc.* **75**, 53 (1979).
- <sup>20</sup>V. E. Bondybey and J. H. English, *J. Chem. Phys.* **69**, 1865 (1978).
- <sup>21</sup>C. R. Quick, Jr., and R. E. Weston, Jr., *J. Chem. Phys.* **74**, 4951 (1981).
- <sup>22</sup>Y. Matsumi, T. Munakata, and T. Kasuya, *J. Chem. Phys.* **81**, 1108 (1984).
- <sup>23</sup>H. J. Hurst, D.Phil. thesis, Oxford University, 1965.
- <sup>24</sup>R. F. Barrow and R. P. du Parcq, in *Elemental Sulphur*, edited by B. Meyer (Interscience, New York, 1965), Chap. 13.
- <sup>25</sup>K. P. Huber and G. Herzberg, *Constants of Diatomic Molecules* (Van Nostrand Reinhold, New York, 1979).
- <sup>26</sup>J. E. Meakin and R. F. Barrow, *Can. J. Phys.* **40**, 377 (1962).
- <sup>27</sup>K. A. Meyer and D. R. Crosley, *Can. J. Phys.* **51**, 2119 (1973).
- <sup>28</sup>P. Patino and R. F. Barrow, *J. Chem. Soc., Faraday Trans.* **78**, 1271 (1982).
- <sup>29</sup>M. Heaven, T. A. Miller, and V. E. Bondybey, *J. Chem. Phys.* **80**, 51 (1984).
- <sup>30</sup>E. Olsson, *Z. Phys.* **108**, 40 (1937).
- <sup>31</sup>G. Herzberg and L. G. Mundie, *J. Chem. Phys.* **8**, 263 (1939).
- <sup>32</sup>G. Herzberg, *Ann. Phys. (Paris)* **15**, 710 (1932).
- <sup>33</sup>B. Rosen, M. Désirant, and J. Duchesne, *Phys. Rev.* **48**, 916 (1935).
- <sup>34</sup>J. M. Ricks and R. F. Barrow, *Can. J. Phys.* **47**, 2423 (1969).
- <sup>35</sup>R. W. Fair and B. A. Thrush, *J. Chem. Soc. Faraday Trans.* **65**, 1208 (1965).
- <sup>36</sup>G. G. Pannetier, P. Goudmand, O. Dessaux, and N. Tavernier, *J. Chem. Phys.* **61**, 395 (1964).
- <sup>37</sup>D. Kley and P. Broida, *J. Photochem.* **6**, 241 (1977).
- <sup>38</sup>W. C. Swope, Y-P. Lee, H. F. Schaefer III, *J. Chem. Phys.* **70**, 947 (1979).
- <sup>39</sup>A. D. Pradhan and H. Partridge, *Chem. Phys. Lett.* **255**, 163 (1996).
- <sup>40</sup>A. O'Keefe and D. A. G. Deacon, *Rev. Sci. Instrum.* **59**, 2544 (1988).
- <sup>41</sup>J. J. Scherer, J. B. Paul, A. O'Keefe, and R. J. Saykally, *Chem. Rev.* **97**, 25 (1997).
- <sup>42</sup>M. D. Wheeler, S. M. Newman, A. J. Orr-Ewing, and M. N. R. Ashfold, *J. Chem. Soc. Faraday Trans.* **94**, 337 (1998).
- <sup>43</sup>J. Pearson, A. J. Orr-Ewing, M. N. R. Ashfold, and R. N. Dixon, *J. Chem. Phys.* **106**, 5850 (1997).
- <sup>44</sup>M. J. Cooper, J. M. F. Elks, and C. M. Western (private communication).
- <sup>45</sup>M. D. Wheeler, A. J. Orr-Ewing, M. N. R. Ashfold, and T. Ishiwata, *Chem. Phys. Lett.* **268**, 421 (1997).
- <sup>46</sup>M. D. Wheeler, A. J. Orr-Ewing, and M. N. R. Ashfold, *J. Chem. Phys.* **107**, 7591 (1997).
- <sup>47</sup>PGOPHER spectral simulation program written by C. M. Western.
- <sup>48</sup>G. Herzberg, *Molecular Spectra and Molecular Structure* (Van Nostrand Reinhold, New York, 1950), Vol. 1, and references therein.
- <sup>49</sup>MOLPRO is a package of *ab initio* programs written by H.-J. Werner and P. J. Knowles, with contributions from J. Almlöf, R. D. Amos, A. Berning, M. J. O. Deegan, F. Eckart, S. T. Elbert, C. Hampel, R. Lindh, W. Meyer, A. Nicklass, K. Peterson, R. Pitzer, A. J. Stone, P. R. Taylor, M. E. Mura, P. Pulay, M. Schuetz, H. Stoll, T. Thorsteinsson, and D. L. Cooper (1996).
- <sup>50</sup>D. E. Woon, K. A. Peterson, and T. H. Dunning, *J. Chem. Phys.* **98**, 1358 (1993), and references therein.
- <sup>51</sup>H.-J. Werner and P. J. Knowles, *J. Chem. Phys.* **89**, 5803 (1988); *Chem. Phys. Lett.* **145**, 514 (1988); H.-J. Werner and E. A. Reinsch, *J. Chem. Phys.* **76**, 3144 (1982); H.-J. Werner, *Adv. Chem. Phys.* **LXIX**, 1 (1987).
- <sup>52</sup>P. J. Knowles and H.-J. Werner, *Theor. Chim. Acta* **84**, 95 (1992).
- <sup>53</sup>H.-J. Werner and P. J. Knowles, *J. Chem. Phys.* **82**, 5053 (1987); P. J. Knowles and H.-J. Werner, *Chem. Phys. Lett.* **115**, 259 (1985). See also H.-J. Werner and W. Meyer, *J. Chem. Phys.* **73**, 2342 (1980); **74**, 5794 (1981).
- <sup>54</sup>*Atomic Energy Levels*, Natl. Stand. Ref. Data Ser., Natl. Bur. Stand. (US), 35/V III (1971).
- <sup>55</sup>M. J. Cooper and C. M. Western, *Chem. Phys. Lett.* **267**, 365 (1997).
- <sup>56</sup>R. J. Le Roy, RKR1, University of Waterloo Chemical Physics Research Report No. CP-425 (1992).
- <sup>57</sup>R. J. Le Roy, LEVEL 6.1, University of Waterloo Chemical Physics Research Report CP-555R (1996).
- <sup>58</sup>M. D. Wheeler, Ph.D. thesis, University of Bristol, 1997.
- <sup>59</sup>R. J. LeRoy, *Comput. Phys. Commun.* **52**, 383 (1989); BCONT 1.4, University of Waterloo Chemical Physics Research Report CP-329R (1993).
- <sup>60</sup>P. S. Julienne and M. Krauss, *J. Mol. Spectrosc.* **56**, 270 (1975).
- <sup>61</sup>J. N. Murrell and J. M. Taylor, *Mol. Phys.* **16**, 609 (1969).
- <sup>62</sup>S. S.-L. Chiu, A. S.-C. Cheung, M. Finch, M. J. Jamieson, K. Yoshino, A. Dalgarno, and W. H. Parkinson, *J. Chem. Phys.* **97**, 1787 (1992).
- <sup>63</sup>H. F. Schaefer III, and W. H. Miller, *J. Chem. Phys.* **55**, 4107 (1971).
- <sup>64</sup>R. F. Barrow, G. G. Chandler, and C. B. Meyer, *Philos. Trans. R. Soc. London* **260**, 395 (1960).
- <sup>65</sup>O. Atabek and R. Lefebvre, *Chem. Phys. Lett.* **17**, 167 (1972).